DOI: 10.1002/anie.200801748

Diffusion in Porous Materials

Quasi-Elastic Neutron Scattering and Molecular Dynamics Study of Methane Diffusion in Metal Organic Frameworks MIL-47(V) and MIL-53(Cr)**

Nilton Rosenbach, Jr., Hervé Jobic, Aziz Ghoufi, Fabrice Salles, Guillaume Maurin,* Sandrine Bourrelly, Philip L. Llewellyn, Thomas Devic, Christian Serre, and Gérard Férey*

Methane is the second most important greenhouse gas with a global-warming impact higher than that of carbon dioxide.[1] Although the level of methane emission is currently stable, after increasing by a factor of two in the last century, its effect on atmosphere pollution is still important. Much effort is concentrated on reducing emissions of this gas in accordance with the Kyoto agreement.[2] On the other hand, methane is the main component of natural gas and an important, clean, and renewable energy source that has significant advantages over gasoline, that is, clean burning, low cost, higher energy per unit mass, and profuse world reserves. However, applications of natural gas have been impeded by its low energy density under economic and safe storage pressures.[3]

Advances in preventing or exploiting methane emissions can provide environmental benefits. Developing new porous materials that can adsorb and store methane is of great current economic interest.[3] In 2006, the U.S. Department of Energy (DOE) set the target for methane storage at 180 v(STP)/v (equivalent volume of methane at standard temperature and pressure per volume of adsorbent material) under 35 bar at room temperature.[4] With this in mind, several porous materials have been evaluated as potential storage media for methane, such as single-walled carbon nanotubes, zeolites, clathrate hydrates, and activated carbon.[5–8] Metal organic framework (MOF) materials, which combine inorganic nodes containing metal centers and organic linker moieties (e.g., carboxylates, phosphonates, imidazolates), are potentially interesting for this purpose, as they combine low framework density and high adsorption capacity.[9–12] Furthermore, the presence of organic moieties within their pore walls can give rise to additional interactions (van der Waals or π–π interactions) with organic probe molecules such as hydrocarbons and aromatics which can enhance the storage capability. Several experimental and theoretical investigations have shown that some MOFs exhibit high CH_4 uptake.[9–13] Significant illustrative examples are the materials MIL-100 and MIL-101, synthesized by Férey et al., which can store much larger amounts of CH_4 than the industrially most widely used NaX zeolite under the same experimental conditions (10 mmol g^{-1} vs. 3.5 mmol g^{-1} at 35 bar).[10,14] Furthermore, in applications involving gas storage, besides high adsorption capacity, a high diffusion rate is also required to avoid a penalizing limitation on the charging/discharging time. In the same way, this kinetic factor is essential for the development of transport-based devices.

Although many studies have been dedicated to the adsorption equilibrium in MOFs, only few computational and experimental studies have been reported on the diffusion of CH_4 in these systems. Sarkisov et al.[15] were the first to report a theoretical investigation of the self-diffusion coefficient D_s of CH_4 in MOF-5. They were followed by Skoulidas and Sholl,[16] who predicted the self-diffusivity behavior of CH_4 for a wide range of loadings in various MOFs including MOF-2, MOF-3, and HKUST-1. More recently, Amirjalayer et al.[17] calculated D_s values of benzene and methane for a given loading in MOF-5 taking into account the flexibility of the framework. Following a similar approach, the self-diffusion coefficient of benzene was also simulated by Greathouse and Allendorf.[18]

From an experimental standpoint, only pulsed field gradient (PFG) NMR diffusion measurements have been reported on various hydrocarbons in MOF-5, including methane at high loading.[19] Quasi-elastic neutron scattering (QENS) measurements have given detailed molecular-level information on the diffusion of various adsorbates in nanoporous materials.[20] More specifically, this experimental tool has proved to be very powerful in investigating the depend-

[*] Dr. H. Jobic
Institut de Recherches sur la Catalyse et l'environnement de Lyon
Université de Lyon, CNRS
2. Av. A. Einstein, 69626 Villeurbanne (France)
Fax: (+33) 4-7244-5399
E-mail: herve.jobic@ircelyon.univ-lyon1.fr
Dr. N. Rosenbach, Jr., Dr. A. Ghoufi, Dr. F. Salles, Dr. G. Maurin
Institut Charles Gerhardt Montpellier
Université Montpellier 2
Place E. Bataillon, 34095 Montpellier cedex 05 (France)
Fax: (+33) 4-6714-4290
E-mail: gmaurin@lpmc.univ-montp2.fr
Dr. S. Bourrelly, Dr. P. L. Llewellyn
Laboratoire Chimie Provence
Universités d'Aix-Marseille I,II et III – CNRS, UMR 6264
Centre de Saint Jérôme, 13397 Marseille (France)
Dr. T. Devic, Dr. C. Serre, Prof. G. Férey
Institut Lavoisier, UMR CNRS 8180
Université de Versailles
Saint-Quentin-en-Yvelines
78035 Versailles Cedex (France)

[**] This work was supported by the French program ANR CO_2 "NoMAC" (ANR-06-CO2-008) and European funding ALFA II "NANOGASTOR" (II-0493-FA-FI). We thank the Institut Laue-Langevin (Grenoble, France) for the neutron beam time, Dr. M. M. Koza for his help, and the CINES for computational facility.

Supporting information for this article is available on the WWW under http://dx.doi.org/10.1002/anie.200801748.

ence on loading of the self- and transport diffusivities for various hydrocarbons in zeolites.[21] Molecular simulations are usually valuable in interpreting QENS experiments and elucidating the diffusion mechanism at the microscopic scale. We have thus combined QENS measurements with molecular dynamics (MD) simulations to investigate the self-diffusivity of CH_4 in MOF-type systems for a wide range of loadings.

The selected MOFs are the MIL-53(Cr^{3+})[22] and MIL-47(V^{4+})[23] systems, which belong to the MIL (Materials of the Institut Lavoisier) series of hybrid porous materials. Isostructural MIL-53(Cr) and MIL-47(V) are built up from infinite chains of corner-sharing $Cr^{3+}O_4(OH)_2$ or $V^{4+}O_6$ octahedra, interconnected by terephthalate groups to create a 3D framework containing 1D diamond-shaped channels with pores of free diameter close to 8.5 Å (Figure 1). In MIL-53(Cr), the hydroxyl groups located at the M-O-M links (μ_2-OH groups) are potential attractive sites for the probe molecules and/or can hinder their mobility. The resulting adsorption/diffusion mechanisms are thus different to those of MIL-47(V), in which these groups are replaced by μ_2-O bridges.

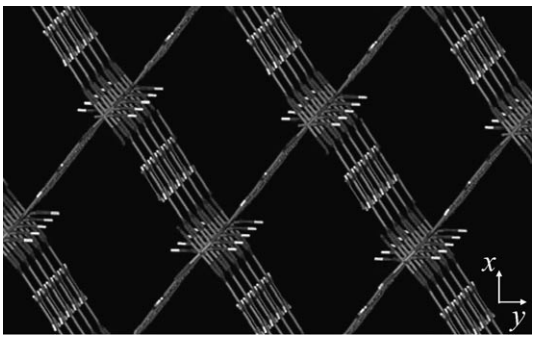

Figure 1. View of the MIL-53(Cr) structure along the chain (*z* axis), highlighting the 1D pore system. The MIL-47(V) structure is obtained by replacing the μ_2-OH groups with μ_2-O groups.

The QENS measurements were performed on the time-of-flight spectrometer IN6 at the Institut Laue-Langevin. The QENS method is mainly used to study hydrogen-containing compounds, because of the large cross section of hydrogen.[21] Since this cross section is essentially incoherent, self-diffusion of the adsorbate is probed. To reduce scattering from the MOFs relative to the adsorbate in the QENS experiments, fully deuterated analogues of MIL-53(Cr) and MIL-47(V) were prepared. Synthesis and activation were performed by using the published procedures[22–24] except that deuterated terephthalic acid was used as a reactant. The hydrogen atoms of the μ_2-OH bridges in MIL-53(Cr) were exchanged with deuterium by stirring in boiling D_2O after activation. On IN6, the incident neutron energy was taken as 3.12 meV, corresponding to a wavelength of 5.1 Å. After scattering by the sample, the neutrons are analyzed as a function of flight time and angle. The wave-vector transfer Q varies with scattering angle and ranged from 0.24 to 1.5 $Å^{-1}$. Spectra from different detectors were grouped in order to obtain reasonable counting statistics and to avoid the Bragg peaks of the MIL frameworks. Time-of-flight spectra were then converted to energy spectra. The line shape of the elastic-energy resolution could be fitted by a Gaussian function, the half-width at half-maximum (HWHM) of which varied from 40 μeV at small Q to 50 μeV at large Q. Four different CH_4 loadings, determined by volumetry during the QENS experiments, were investigated for both MIL-47(V) and MIL-53(Cr).

The QENS spectra recorded at 230 K for the second loading are reported in Figure 2 for one selected Q value. The

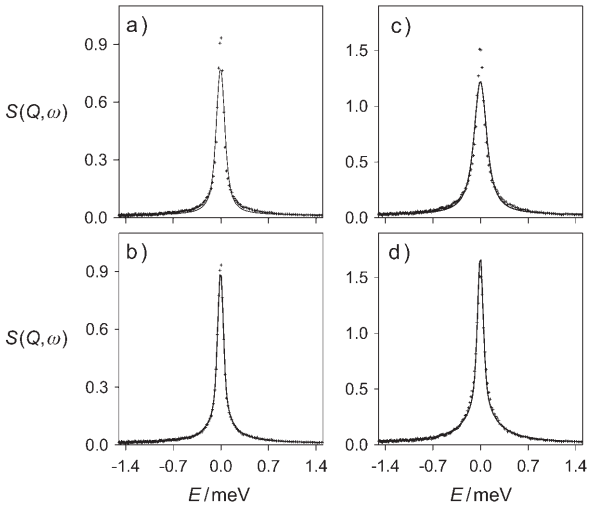

Figure 2. Comparison between experimental (•••••) and fitted (——) QENS spectra obtained for CH_4 in a, b) MIL-53(Cr) for 1.1 molecules per u.c., c, d) MIL-47(V) for 1.6 molecules per u.c. The solid lines correspond to a, c) 3D diffusion and b, d) 1D diffusion ($T = 230$ K, $Q = 0.35$ $Å^{-1}$, u.c. = unit cell).

measured intensities are presented in terms of the dynamical structure factor $S(Q,\omega)$, where $\hbar Q$ and $\hbar\omega$ are the momentum and energy transfers, respectively. The spectra were first fitted individually with three- or one-dimensional diffusion, and then convoluted with isotropic rotation and instrumental resolution. The dynamical structure factor must be powder-averaged for 1D diffusion, which results in a shape different from a typical Lorentzian function for 3D diffusion.[25] Comparison between experimental and calculated profiles (Figure 2) shows that 1D diffusion fits better the experimental data in both MIL systems. The same observation was made for the whole range of investigated CH_4 loadings. It shows that the CH_4 displacements along the x and y directions in a given tunnel are negligible. This implies that no CH_4 motion occurs between two neighboring channels through the phenyl rings, which might be suspected if these rings reorientate perpendicular to the $Cr(OH)_2O_4$ moiety. Furthermore, the spectra shown in Figure 3 indicate that unidirectional diffusion is also valid at all temperatures, and that the influence of temperature is larger in MIL-53(Cr) than in MIL-47(V). Since the quasi-elastic broadening is related to the diffusivity, a simple visual inspection of the spectra shows that D_s varies more with temperature in MIL-53(Cr), so the activation energy for CH_4 diffusion will be higher in that structure.

One-dimensional self-diffusion coefficients were derived from the low-Q range; the lowest Q value of 0.27 $Å^{-1}$

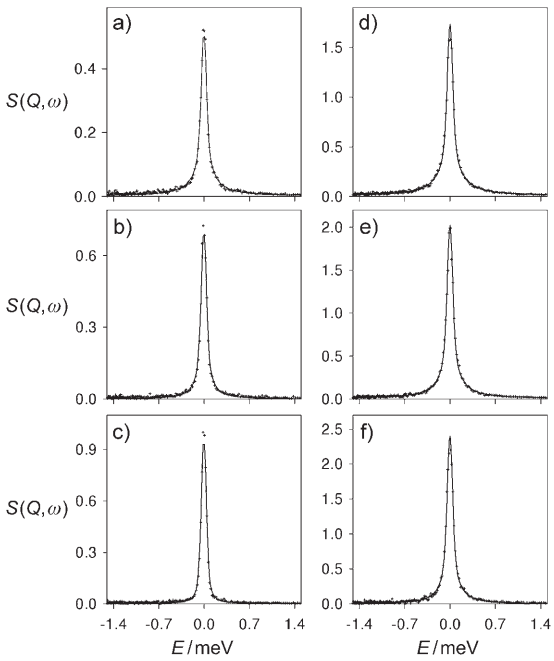

Figure 3. QENS spectra obtained for CH_4 in MIL-53(Cr) at a) 230, b) 200, and c) 170 K for a concentration of 1.1 molecule per u.c.; the spectra were fitted to 1D diffusion. Corresponding spectra for MIL-47(V) are reported in d)–f) for 1.6 molecules per u.c. ($Q = 0.27$ Å^{-1}).

corresponds to a length scale of 23.3 Å in real space. This distance is much larger than the unit-cell parameter along the direction of the tunnel (6.8 Å), so that Fickian behavior can be observed. Figure 4 shows the orientationally averaged self-diffusion coefficients ($D_s = D_{1D}/3$) for both MIL-47(V) and MIL-53(Cr) at 230 K, defined within an error bar of 20% over the whole range of loading. Self-diffusion coefficients were also extracted by using a 1D jump-diffusion model with a Gaussian distribution of jump lengths along the channels. The resulting diffusivities were systematically larger, but the number of spectra was too limited to determine the parameters of the model with reasonable accuracy (depending on the loading, the mean jump lengths obtained with this model range between 5 and 10 Å).

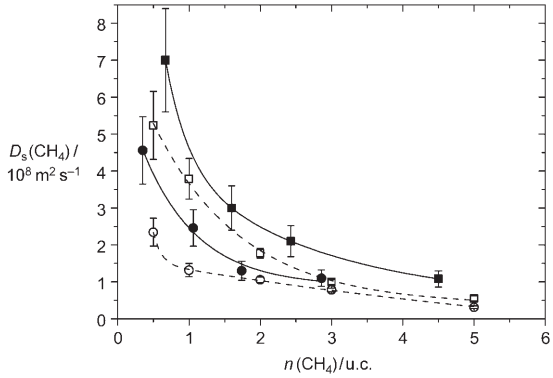

Figure 4. Self-diffusion coefficients D_s for MIL-47(V) (squares) and MIL-53(Cr) (circles) as a function of loading: QENS at 230 K (full symbols and solid lines), MD at 250 K (empty symbols and dashed lines). The error bars are reported for both simulations and QENS experiments.

It appears from Figure 4 that methane diffusivities are significantly higher in MIL-47(V) than in MIL-53(Cr) over the whole range of investigated loadings. This observation is consistent with the trend observed for the activation energy E_a measured for similar loadings: 3.0 and 8.0 kJ mol^{-1} for MIL-47(V) and MIL-53(Cr), respectively. One can thus assume that the μ_2-OH groups in MIL-53(Cr) act as attractive sites and steric barriers, and both effects contribute to perturbing the trajectory and thus decreasing the mobility of CH_4. Comparable values of E_a were reported for methane in ZSM-5 and NaY zeolites: 4.7 and 6.3 kJ mol^{-1}.[26] Furthermore, in both MILs, CH_4 exhibits very high mobility, as highlighted by the large D_s value observed at low loading (Figure 4). Such a phenomenon has never been observed for methane in other MOFs, in which only a monotonous decrease of D_s was found,[16] while a similar sudden increase in D_s at low loading for H_2 and CH_4 was previously predicted by Skoulidas et al. in single-walled carbon nanotubes.[27] By using an arbitrary analytical expression to fit the experimental data of MIL-47(V) reported in Figure 4, it is possible to estimate the D_s value at infinite dilution to be at least $(3.0 \pm 0.6) \times 10^{-7}$ m^2 s^{-1} at 230 K. From the experimental activation energy, one can thus obtain a D_s value of about $(4.2 \pm 0.8) \times 10^{-7}$ m^2 s^{-1} at room temperature, which is more than one order of magnitude higher than that observed in AlPO-5[25] and NaY zeolite of similar pore size.[26] Compared with MOF-5, this self-diffusion coefficient is about one order of magnitude higher than those predicted at low loading,[15,16] while it is only slightly larger than that extracted by PFG NMR measurements (1.7×10^{-7} m^2 s^{-1}).[19] On the timescale of the QENS experiments, the molecules remain inside the crystals, so a single methane species is observed with this technique, whereas they diffuse within and between the crystals on the PFG NMR timescale.

To more deeply understand the diffusion mechanism of CH_4 on the microscopic scale, molecular dynamics (MD) simulations were performed for both MILs. These calculations were based on atomistic interatomic potential parameters and DFT-derived partial charge models for the MIL frameworks (Table S1, Supporting Information). CH_4 was represented by an explicit model in which each constituting atom is charged and considered as a Lennard–Jones center with parameters taken from previous investigations.[28] While the adsorbate was treated as fully flexible by means of two-body bond stretches and three-body angle potentials by using the parameters of Oie et al.[29] (Table S2, Supporting Information), the MIL frameworks were maintained rigid. This latter approximation is supported by our previous in situ X-ray diffraction study, which showed that the MIL structures do not undergo any significant modification over the whole range of investigated CH_4 loading.[30] For the interactions between CH_4 and the organic moiety, the CH_4 parameters were combined with those taken from the widely used Dreiding force field,[31] by using Lorentz–Berthelot mixing rules, whereas the CH_4/inorganic node interaction was treated by our previous ab initio derived force field.[28] From a fair agreement between the simulated thermodynamics data and those collected by microcalorimetry on both MIL systems for a wide range of pressure (see the Supporting Information), it

was possible to validate these sets of potential parameters (Table S2, Supporting Information).

The MD simulations were then performed at 250 K in the NVT ensemble by using the Evans isokinetic ensemble. The simulation box consisted of 16 unit cells (u.c.) containing 1152 and 1216 atoms for MIL-47(V) and MIL-53(Cr), respectively, loaded with 8, 16, 32, 48 and 80 CH_4 molecules to be consistent with the experimentally investigated loadings. The calculations were then performed for these different loadings, each for 2×10^6 steps (i.e., 2 ns) with a time step of 1 fs, following 0.5 ns of equilibration. Details of the MD simulations are provided in the Supporting Information. From the mean-square displacement (MSD) curves averaged over multiple time origins and five different MD trajectories (Figure S4, Supporting Information), it was thus possible to extract the self-diffusion coefficient D_S according to the Einstein relation. An estimate of the statistical error on D_s was determined for each loading from the standard deviation of the average value obtained from the five MD trajectories. As shown in Figure 4, the simulated values of D_s for both MILs are in fair agreement with those measured by QENS for intermediate and high CH_4 loadings. Moreover, in the domain of low loading, our simulations reproduce very well the enhanced mobility of MIL-47(V), while they fail to capture the magnitude of the D_s increase for MIL-53(Cr). Our calculations confirm a slower diffusion process in MIL-53(Cr), consistent with the calculated residence times for CH_4, which are longer around the μ_2-OH groups than near the μ_2-O groups in MIL-47(V). As plotted in Figure S5 (Supporting Information), the mean values are 5.4 and 3.3 ps in MIL-53(Cr) and MIL-47(V), respectively. This trend explains the higher experimental activation energy measured for MIL-53(Cr). Furthermore, the drop in D_s when the loading increases is due to an increased number of collisions between CH_4 molecules.

To gain some insight into the microscopic diffusion mechanism, the probability density of methane in the pore of both MILs was calculated from the analysis of the configurations stored during the MD runs at 250 K. The resulting 2D density plots obtained at low loading are shown in Figure 5. They clearly show that the positions of CH_4 with the highest probability in the pore of MIL-53(Cr) (Figure 5a) are centered around the μ_2-OH groups. In MIL-47(V) (Figure 5b), a broader probability distribution within the pore is obtained, but the regions around the μ_2-O groups remain the most favorable. One observes the same behavior in the whole range of investigated loadings. These spatial arrangements are consistent with those obtained from our grand canonical Monte Carlo simulations (Figure S3, Supporting Information) which also provided the strength of the interaction by means of the adsorption enthalpy of 15.6 and 17.9 kJ mol^{-1} for MIL-47(V) and MIL-53(Cr), respectively.

Two-dimensional free-energy maps through the *xz* plane of a given tunnel were then calculated at high loading (5 CH_4/u.c.) for both MILs by the histogram sampling method[32] (Figure 6). They show that in MIL-53(Cr) (Figure 6a), the lower-energy regions are centered around the μ_2-OH groups as well as in the middle of the pore. In MIL-47(V), this latter region is much more favorable for the CH_4 molecules. Furthermore, minimum-energy pathways of CH_4 in the pores of both MILs can be approximately drawn by following the lower parts of the 2D free-energy maps (Figure 6). They are predominantly orientated along the direction of the tunnel and thus confirm a 1D diffusion mechanism in both cases. In MIL-53(Cr) (Figure 6a), one can imagine a sequence of jumps between two consecutive μ_2-OH groups. This observation suggests that the diffusion of CH_4 is mainly ruled by the presence of the μ_2-OH groups, which leads to 1D diffusion along the tunnel of the pore, while the displacements along the *x* and *y* directions are negligible. CH_4 can also diffuse along the *z* axis by following a pathway centered

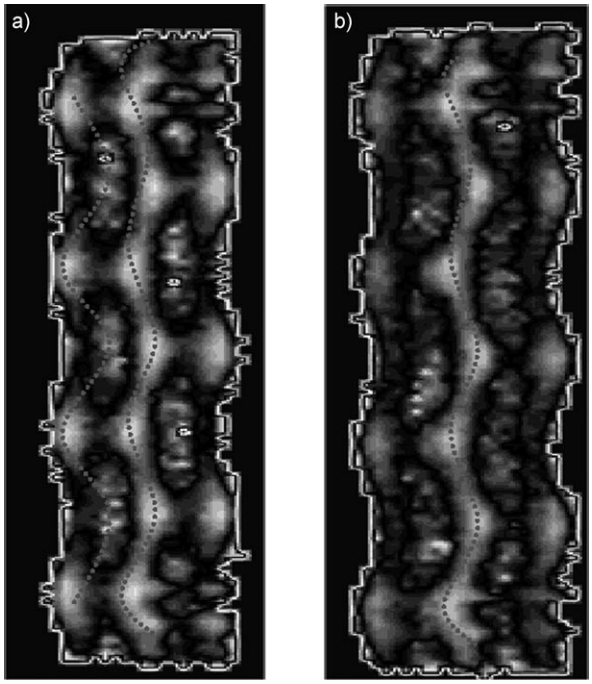

Figure 6. 2D free-energy maps of methane in a) MIL-53(Cr) and b) MIL-47(V) at 250 K obtained through the *xz* plane of a given tunnel for a loading of five CH_4 molecules per u.c. White corresponds to regions of lower free energy, and black to regions of higher free energy. The dashed lines are guides to the eye.

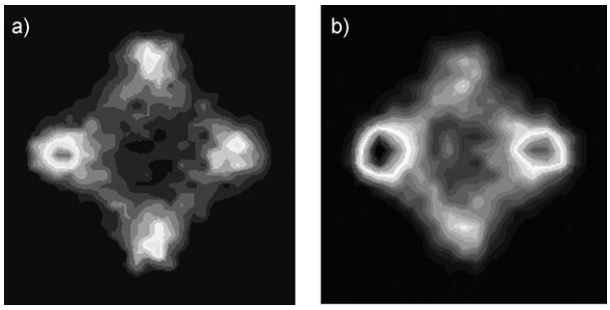

Figure 5. 2D density plots of the distribution of methane in a) MIL-53(Cr) and b) MIL-47(V) at 250 K obtained through the *xy* plane. White regions have a higher probability of containing CH_4 molecules; black regions correspond to unfavorable positions. These data were calculated for one CH_4 molecule per u.c.

around the middle of the pore. As MIL-47(V) does not have μ_2-OH groups, one would imagine a 3D diffusion mechanism with random motions within the pore of the material. However, due to its large kinetic diameter and weak interactions with both the μ_2-O groups and the organic linkers, the displacements of CH_4 are mainly restricted to the direction of the tunnel, as shown in Figure 6b, with motion mainly centered in the middle of the pore. These constrained motions thus lead to a global 1D diffusion mechanism. Further, we have observed that this behavior is even more valid at higher loading, where the interactions between the probe molecules tends to enhance the predominance of the unidirectional diffusion along the *z* axis by restricting the motions in the *x* and *y* directions.

The microscopic mechanisms elucidated in both MILs support the use of a 1D diffusion model to fit the QENS spectra (Figure 2). Furthermore, at low loading it is possible to estimate mean jump lengths of 5.6 and 8.1 Å associated with characteristic time intervals of 7.3 and 6.0 ps in MIL-53(Cr) and MIL-47(V), respectively. These distances are within the range of jump lengths extracted by QENS and are similar to the distances separating two consecutive μ_2-O and μ_2-OH groups in MIL-47(V) and MIL-53(Cr), respectively. Moreover, our simulations show a broad distribution of jump lengths, which is consistent with the QENS observations.

In summary, our joint QENS experiment/MD simulation approach has proved to be a valuable tool for elucidating the diffusion mechanism of CH_4 in MOF-type materials. High mobility was found at low loading with a self-diffusion coefficient at infinite dilution much higher than those observed in other MOFs and zeolites with large pores such as NaY. Furthermore, it was possible to show that the global diffusion mechanism of CH_4 does not strongly depend on the chemical features of the MOF material. A 1D diffusion model corresponding to motion of CH_4 along the tunnel was thus observed in both MIL materials. This methodology, which is able to probe the dynamics of a large number of gases, including H_2,[33] in MOF materials, is an essential complementary tool for the further development of MOFs in gas storage, as these processes are generally governed not only by thermodynamic criteria but also by transport-kinetic properties.

Received: April 15, 2008
Revised: May 20, 2008
Published online: July 24, 2008

Keywords: diffusion · metal–organic frameworks · methane · molecular dynamics · neutron diffraction

[1] K. Zhang, U. Kogleschatz, B. Eliasson, *Energy Fuels* **2001**, *15*, 395.
[2] B. Hileman, *Chem. Eng. News* **2004**, *82*, 26, 44.
[3] A. Celzard, V. Fierro, *Energy Fuels* **2005**, *19*, 573.
[4] J. Wegrzyn, M. Gurevich, *Appl. Energy* **1996**, *55*, 71.
[5] P. D. Rolniak, R. Kobayashi, *Am. Inst. Chem. Eng. J.* **1980**, *26*, 616.
[6] A. A. Khokhar, J. S. Gudmundsson, E. D. Sloan, *Fluid Phase Equilib.* **1998**, *150–151*, 383.
[7] D. F. Quinn, J. A. F. MacDonald, *Carbon* **1992**, *30*, 1097.
[8] V. C. Menon, S. J. Komarneni, *J. Porous Mater.* **1998**, *5*, 43.
[9] S. Ma, D. Sun, J. M. Simmons, C. D. Collier, D. Yuan, H.-C. Zhou, *J. Am. Chem. Soc.* **2008**, *130*, 1012.
[10] P. L. Llewellyn, S. Bourrelly, C. Serre, A. Vimont, M. Daturi, L. Hamong, G. De Weireld, J. S. Chang, D. Y. Hong, Y. K. Hwang, S. H. Jhung, G. Férey, *Langmuir* **2008**, *24*, 7245.
[11] A. C. Sudik, A. R. Millward, N. W. Ockwig, A. P. Côté, J. Kim, O. M. Yaghi, *J. Am. Chem. Soc.* **2005**, *127*, 13519.
[12] W. Zhou, H. Wu, M. R. Hartman, T. Yildirim, *J. Phys. Chem. C* **2007**, *111*, 16131.
[13] S. Wang, *Energy Fuels* **2007**, *21*, 953.
[14] S. Y. Zhang, O. Talu, D. T. Hayhurst, *J. Phys. Chem.* **1991**, *95*, 1722.
[15] L. Sarkisov, T. Duren, R. Q. Snurr, *Mol. Phys.* **2004**, *102*, 211.
[16] A. I. Skoulidas, D. S. Sholl, *J. Phys. Chem. B* **2005**, *109*, 15760.
[17] S. Amirjalayer, M. Tafipolsky, R. Schmid, *Angew. Chem.* **2007**, *119*, 467; *Angew. Chem. Int. Ed.* **2007**, *46*, 463.
[18] J. A. Greathouse, M. D. Allendorf, *J. Phys. Chem. C* **2008**, *112*, 5795.
[19] F. Stallmach, S. Groger, V. Kunzel, J. Karger, O. M. Yaghi, M. Hesse, U. Muller, *Angew. Chem.* **2006**, *118*, 2177; *Angew. Chem. Int. Ed.* **2006**, *45*, 2123.
[20] H. Jobic, D. N. Theodorou, *Microporous Mesoporous Mater.* **2007**, *1–3*, 21.
[21] H. Jobic, N. Laloue, C. Laroche, J. M. Van Baten, R. Krishna, *J. Phys. Chem. B* **2006**, *110*, 2195.
[22] C. Serre, F. Millange, C. Thouvenot, M. Nogués, G. Marsolier, D. Louer, G. Férey, *J. Am. Chem. Soc.* **2002**, *124*, 13519.
[23] K. Barthelet, J. Marrot, D. Riou, G. Férey, *Angew. Chem.* **2002**, *114*, 291; *Angew. Chem. Int. Ed.* **2002**, *41*, 281.
[24] C. Serre, S. Bourrelly, A. Vimont, N. Ramsahye, G. Maurin, P. L. Llewellyn, M. Daturi, Y. Filinchuk, O. Leynaud, P. Barnes, G. Férey, *Adv. Mater.* **2007**, *19*, 2246.
[25] H. Jobic, K. Hahn, J. Kärger, M. Bée, A. Tuel, M. Noack, I. Girnus, G. J. Kearley, *J. Phys. Chem. B* **1997**, *101*, 5834.
[26] H. Jobic, M. Bée, G. J. Kearley, *J. Chem. Phys.* **1994**, *98*, 4660.
[27] A. I. Skoulidas, D. M. Ackerman, J. K. Johnson, D. S. Sholl, *Phys. Rev. Lett.* **2002**, *89*, 185901.
[28] G. Maurin, P. L. Llewellyn, R. G. Bell, *Microporous Mesoporous Mater.* **2006**, *89*, 96.
[29] T. Oie, T. M. Maggiora, R. E. Christoffersen, D. J. Duchamp, *Int. J. Quantum Chem. Quantum Biol. Symp.* **1981**, *8*, 1.
[30] P. L. Llewellyn, G. Maurin, Th. Devic, S. Loera, N. Rosenbach, C. Serre, S. Bourrelly, P. Horcajada, G. Férey, *J. Am. Chem. Soc.*, accepted.
[31] S. L. Mayo, B. D. Olafson, W. A. Goddard III, *J. Phys. Chem.* **1990**, *94*, 8897.
[32] E. Beerdsen, B. Smit, D. Dubbeldam, *Phys. Rev. Lett.* **2004**, *93*, 248301.
[33] F. Salles, H. Jobic, G. Maurin, M. M. Koza, P. L. Llewellyn, T. Devic, C. Serre, G. Férey, *Phys. Rev. Lett.* **2008**, *100*, 245901.

